Antimycobacterial Activity, Phytochemical Profile, and Molecular Docking of Compounds of *Albizia Zygia* (Dc.) J.F. Macrb

Kehongo Moses Nyanguru[a,b], Ephantus Githui Ndirangu[e], Robi Chacha[d], Bakari Chaka,[a], Jones Moody[b], Elizabeth Kigondu[c]

[a]Department of Mathematics and Physical Sciences, School of Pure, Applied and Health Sciences, Maasai Mara University, Narok, Kenya; [b]Department of Medicinal Plant Research and Drug Development, Pan African University Life and Earth Sciences Institute (Including Health and Agriculture)-University of Ibadan, Ibadan, Nigeria; [c]Centre for Traditional Medicine and Drug Research, Kenya Medical Research Institute, Nairobi, Kenya; [d]Centre for Respiratory Disease Research, Kenya Medical Research Institute, Nairobi, Kenya; [e]Department of Physical and Biological Sciences, Murang'a University of Technology, Murang'a, Kenya.

Correspondence to Kehongo Moses Nyanguru (kehongomoses1995@gmail.com)

ABSTRACT

Background: Tuberculosis (TB) remains a significant global health burden, exacerbated by increasing multidrug resistance. Medicinal plants, such as *Albizia zygia* (DC.) J.F. Macbr, is being used in Kenya to manage TB symptoms; however, antimycobacterial potential remains scientifically underexplored.

Methods: The root bark of A. zygia was sequentially extracted using hexane, dichloromethane, ethyl acetate, methanol, and water. Antimycobacterial activity against *Mycobacterium smegmatis* was assessed using the Microplate Alamar Blue Assay (MABA). Cytotoxicity was evaluated via the MTT assay on Vero cells, and synergistic interactions with rifampicin (RIF) were determined using a checkerboard assay. GC-MS was employed for phytochemical profiling, followed by molecular docking against *Mycobacterium tuberculosis* targets (pks13 and EthR) using Schrödinger 2023. ADME/T properties were also predicted using in silico studies.

Results: Methanol and aqueous extracts showed antimycobacterial activity with MIC_{99} values of 625 μg/mL and 2500 μg/mL, respectively, and were non-cytotoxic (CC_{50} >1000 μg/mL), except for the moderately cytotoxic dichloromethane extract. Synergistic and additive interactions with RIF were observed with FICI of 0.5 and 0.63, respectively. GC-MS identified 42 compounds; among which 7-ethyl-quinoline, diphenyl sulfone, hexa-decanoic acid, and 2,4-di-tert-butylphenol have been reported to exhibit antimycobacterial activity, also showed strong binding affinities (d-score ≥ -7.0 kcal/mol) to the multidrug resistance TB protein targets, Pks13 and EthR, suggesting their potential contribution to the observed antimycobacterial effects. ADME/T predictions indicated good oral bioavailability but raised concerns about CYP interactions and short terminal half-lives.

Conclusion: *A. zygia* root bark contains bioactive phytochemicals with promising antimycobacterial activity and synergism with rifampicin. These findings validate the ethnomedicinal use of *A. zygia* in TB management in Kenya; therefore, further in vivo evaluation and pharmacokinetic optimization of lead compounds are needed.

BACKGROUND

Tuberculosis (TB) is among the leading chronic diseases in the world, ranked among the top ten diseases affecting humans, particularly due to the emergence and spread of multidrug-resistant strains.[1] TB is caused by *Mycobacterium tuberculosis* (*Mtb*), which infects the lungs; however, it can also infect other organs such as the spine, kidneys, and brain.[1] According to the World Health Organization (WHO), 2 billion (25%) of the world population in 2020 were infected with TB, with approximately 1.4 million mortalities.[2] The thirty high-burden countries contributed to 86% of TB-reported cases globally. However, half of the 30 high-burden countries are in Africa[3], accounting for more than a quarter of all TB deaths worldwide.[3] Regarding the Ministry of Health (MOH) of Kenya, the TB incidence per 100,000 Kenyans decreased by 3.0% between 2019 and 2020, however, there was a notable increase in MRD-TB.[4] Therefore, there is an urgent need for new, effective, and affordable antimycobacterial agents from both natural and synthetic sources.

Medicinal plants remain a valuable source of therapeutic agents in various indigenous knowledge systems for the treatment of human diseases.[5] It is estimated that out of 250,000 recorded higher plants, 80,000 species are sources of materials for folk medicine and the herbal industry.[6] In addition, fungi, algae, and animals are also utilized.[7] Over 80% of African communities depend on traditional medicine to treat both chronic and acute diseases.[8,9] In the East African region, more than 195 medicinal plant species are reported to be in use for the treatment of TB and MDR-TB.[10] However, only approximately 30 (16%)

have been evaluated for antimycobacterial activity, and even fewer were subjected to phytochemical isolation of active principles. *Albizia zygia* (DC.) J.F. Macrb, a Kenyan indigenous plant, is used in the treatment of TB. Antimycobacterial activity, on the other hand, has not been established.[11–13]

Albizia zygia is a deciduous tree with a spreading crown and elegant architecture, growing in the tropical regions of Eastern, Central, and Western Africa. It belongs to the Fabaceae family and the Albizia genus.[14] In traditional medicine, the bark of *A. zygia* is considered an antidote, aphrodisiac, heat-clearing, emphysema, and deworming. An infusion of *A. zygia* is used to manage various conditions, including pulmonary disorders such as tuberculosis and chronic cough, as well as non-pulmonary conditions like malaria and sterility in women. To alleviate a cough, the crushed root is used as an expectorant and added to food.[15,16] Eye diseases are treated by applying sap from the bark to the eyes. When dried and ground into a powder, the root and stem barks, and leaves of *A. zygia* are applied to wounds, toothaches, yaws, and sores, and a decoction is used to treat diarrhea and fever.[17] Anti-inflammatory, antioxidant[18], antibacterial[15] and anti-cancer properties [19] have also been attributed to *A. zygia* extracts.

Despite its widespread traditional use, the antimycobacterial properties of *A. zygia* remain scientifically underexplored. Therefore, the current study evaluated antimycobacterial activity, cytotoxicity, phytochemicals, drug combination studies, molecular docking against key *Mtb* targets, and ADMET studies of GC-MS-detected phytochemicals.

METHODS AND MATERIALS
Plant Materials
The *A. zygia* plant was identified by Dr. Wanjohi B. K (a plant taxonomist). The root bark was collected from the wild in the Kadate village, Nyando Sub-County, Kisumu County, Nyanza region (coordinates: -0.1801597, 34.8328252). The collected plant materials were placed in a sterile bag and transported to the Kenya Medical Research Institute (KEMRI), Center for Traditional Medicine and Drug Research (CTMDR) for drying. The prepared voucher specimen (WME/1/22/001) was submitted to the herbarium at the University of Eldoret. The plant materials were sliced into small pieces. At room temperature (23±2°C) the plant materials were air-dried for about four weeks to constant weight. An electric mill was used to grind the plant materials into a fine powder (Christy 8 MILL, Serial No. 51474). The fine powder was then packed, labeled, and stored in a moisture-free region, awaiting extraction procedures.[20]

Extraction
Organic Extraction
Plant materials were subjected to serial successive (sequential) extraction by a simple maceration method with organic solvents of increasing polarity (non-polar to polar); [21]. Using a digital analytical balance (Ohaus, Model No PA224), 500 g of *A. zygia* root bark powder was weighed and soaked in 2000 mL of n-hexane with shaking periodically for 2 days. The resulting solvent extract was filtered with No. 1 Whatman filter paper. The residue plant material was reextracted with the same solvent (n-hexane) for 1 day, filtered, and combined with the

previous filtrate. The resulting extract was concentrated using a rotary evaporator (BUCHI Labortechnik AG, 9230, Model No. R-300 EL, Serial No. 1100033194), and transferred to a pre-weighed and labeled vial. The extract was allowed to dry at room temperature for 14 days. Using the extraction technique as for n-hexane, the resultant residue was dried and reextracted with dichloromethane (DCM), then ethyl acetate (EtOAc), and lastly methanol (MeOH) [21]. The percentage yielded was calculated for each extract as follows :

$$\text{Percentage extracted} = \left(\frac{Mass\ of\ crude\ extract}{Mass\ of\ plant\ material} \right) \times 100\% \qquad (1)$$

Aqueous Extraction
Water extraction was performed on the fresh powdered plant materials. 50.0 g of powdered *A. zygia* root bark was mixed with 350 mL of deionized water, and gently heated in a water bath (Model No. 811099, Schutzart DIN 40050-IP20) at 70°C for about 2 hours. The cooled mixture was filtered using cotton wool, followed by a Whatman filter paper No. 1. The resulting filtrate was placed in a flask with a circular bottom. The flask was coated with dry ice (frozen CO_2), mixed with acetone, and then attached to a freeze-drying machine (Butchi, LYOVAPOR L-300) for approximately 24 hours until the aqueous extract was well dried. The dried extract was placed into a pre-weighed vial. All extracts were stored in hermetically sealed vials at 4 °C.[21]

Cytotoxicity
The MTT assay was used for the evaluation of cytotoxicity of the *A. zygia* root bark extracts, a method previously described by Mosmann (1983) with minor modifications [22]. The growth media (10%) and the maintenance media (MM) (25%) were prepared. The African green monkey Vero cells (P18) were grown to confluence, achieved by sub-culturing pregrown cells at 5% CO_2, 98% humidity, and 37°C, for 24 hours at the culture laboratory, CTMDR, KEMRI.

The cells were trypsinized, enumerated using a microscope, and regrown until the desired seeding density of 2.0×10^5 cells/100 µL was achieved. 100 µL of the cells were seeded into the wells of 96-well microplates except for the wells that were used as blanks, where the media was added instead, followed by incubation at 37°C for 24 hours at 5% CO_2, 80% humidity. The plate setting was that after two columns, the media alone was added alone (blank), allowing each plate to be capable of four independent experiments.

A stock solution of 10 mg/mL, 10% DMSO plant extract, and a standard reference drug was prepared. In the plates that were incubated for 24 hours, 35 µL of MM was added, followed by the addition of 15 µL of plant extract in all wells in row H except the blanks (3rd, 6th, 9th, and 12th wells). Serial dilution was carried out from row H to row B (A three-fold dilution), representing 1000, 333.33, 111.11, 37.04, 12.35, 4.12, and 1.37 µg/mL. Row A served as a positive control (No treatment). The 96-well plates were sealed with parafilm and incubated under the same conditions for 48 hours. 10 µL of 5 mg/mL MTT dye was added to all wells, followed by incubation for 4 hours without shaking. Aspiration of the liquid from the wells was performed and 100 µL DMSO was added. An anti-TB

drug, rifampicin (RIF) was used as a standard reference drug. The test was performed in triplicate. The plate reader Enzyme-Linked Immunosorbent Assay (ELIZA) was used to determine the absorbance (at a wavelength of 540 nm and 720 nm). The percentage of living cells at various test concentrations was determined using the following formula:

$$\% \text{ Cell live (cell viability)} = \left(\frac{At - Ab}{Ac - Ab}\right) \times 100\% \qquad (2)$$

At is for the test sample absorbance value, Ab is for the blank absorbance value, and Ac is for the positive control absorbance value. Using free software from AAT Bio quest (https://www.aatbio.com/tools/ic50-calculator), the cytotoxic concentration of test drug samples that caused a 50% reduction in Vero cells (CC_{50} value) was estimated.[23]

In vitro Antimycobacterial Assay

Mycobacterium smegmatis (Msm) was used in this study because it is a non-pathogenic mycobacterium that belongs to the same genus as *Mtb;* however, it is more resistant and comparable to multidrug-resistant TB (MDR-TB).[24,25] Minimum Inhibitory Concentrations (MIC_{99}) for the five extracts were determined using Microplate Alamar Blue Assay (MABA), the method described by Collins & Franzblau (1997) and Webster (2010)[26,27] with slight modification. Middlebrook 7H9 media with ADC/OADC enrichment was used to prepare the plant extract and RIF stock solution at 10 mg/mL 0.2 mg/mL, respectively. The stock solution was stored at 4 °C waiting for antimycobacterial activity.

Inoculum Preparation of *Mycobacterium smegmatis (Msm)*

A pre-cultured non-pathogenic reference strain of *Msm* ATCC607 was prepared from the preexisting seed stock at the Centre for Respiratory Diseases Research (CRDR), KEMRI. A dilution ratio of 1:500 was performed in the pre-cultured *Msm* with an Optical density at a wavelength of 600 nm (OD_{600}) of 0.6-0.8 (logarithmic phase).[26,27]

Broth Microdilution Method

Minimum inhibitory concentration (MIC_{99}) was determined using a two-fold serial dilution method. Briefly, to each well in the 96-well microtiter plate, 50 µL of 7H9 media was added, except wells B, C, D, E, F, and G in the 1st column. Each test extract and RIF were tested in duplicate, with A and B rows representing the negative control. In the first column, 100 µL of the tested samples were placed in wells C, D, E, and F, while the RIF in wells G and H. A serial dilution (Two-fold) was performed by transferring 50 µL of the 1st well content to the next well, until the last well (well in the 12th column), whereby the last 50 µL was discarded. To all wells, 50 µL of pre-cultured *Msm* was added with the exception of row A and B wells. The plates were sealed using parafilm paper to avoid evaporation, and placed in a tight box, incubated at 37°C for 48 hrs. 20 µL of 0.01% fresh resazurin blue dye was added in each well and incubated for another 24 hrs. The conversion of blue to pink colour demonstrated the non-inhibition of *Msm* (The test drug was inactive), while the blue persistence demonstrated the inhibition of microorganisms' growth (activity of test plant extracts

against *Msm)*. Each test drug samples were performed in triplicate.[26,27]

Antimycobacterial Synergistic Activity (Checkerboard assay)

A drug combination study of the methanolic and aqueous extracts with RIF was carried out based on a 2-dimensional checkerboard according to Hsieh (1993) with slight modification.[28] 0.2 mg/mL RIF and 5 mg/mL extract stock solution were used. In the 96-well microplate (plate A), 50 µL Middlebrook 7H9 broth media was added to each well except for the 1st and 2nd columns, while 100 µL of RIF was added in the 2nd column wells. Two-fold serial dilution was performed. In a different 96-well microplate (plate B), 50 µL of 7H9 broth media was added to all wells, except for wells in rows A and B, while 100 µL of plant extract was added to row B wells. Serial dilution (two-fold) was also performed. The content of plate A (RIF, horizontally two-fold dilution) was overlaid into plate B (plant extract vertically two-fold dilution). In the first well, first column, 50 µL of the media was added and served as the negative control. 100 µL of *Msm* was added to all wells except for the 1st column and row A, whereby 50 µL was added. The plates were sealed with parafilm and incubated for 48 hours at 37 ℃. 20 µL of 0.02% resazurin dye was added to all wells, sealed with parafilm, and further incubated for 24 hours. Wells in the 1st column gave the MIC_{99} of the plant extract while the wells in row A gave the MIC_{99} of RIF.

Synergistic interaction was determined through the estimation of the fractional inhibitory concentration (FIC) and fractional inhibitory concentration index (FICI) values, using the formula:

$$(FICI) = \frac{MIC \text{ of } A \text{ (in combination with B)}}{MIC \text{ A tested singly}} (FIC \text{ of } A) + \frac{MIC \text{ of } B \text{ (in combination with A)}}{MIC \text{ B tested singly}} (FIC \text{ of } B)$$
$$(3)$$

Phytochemical screening of bioactive extracts

Methanolic and aqueous extracts were subjected to qualitative phytochemical screening for the detection of the secondary metabolites present using standard methods previously described by Harborne (1984)[29] with minor modifications.

Gas Chromatography Mass-Spectrometry (GC-MS) Analysis Solid Phase Extraction (SPE)

In a 15-mL centrifuge tube, 3 mg of methanolic and aqueous extracts were added, followed by the addition of 6 mL of analytical-grade methanol. The extracts were sonicated for 30 minutes (Model No. GT-Sonic D9, from GT-Sonic Technology, Meizhou, Guangdong, Japan), and filtered with Whatman No. 1 filter paper. The filtrate was subjected to the SPE procedure for purification. The SPE cartridge (Agilent Bond Elut C18) was set manually to a flow rate of about 1 mL/min in the SPE manifold. The analytes were eluted with 6 mL of 100% analytical-grade methanol, followed by hexane. The eluents were reconstituted for 45 minutes at 40 ℃ in a DNA concentrator (Model No.: DNA-23050-A00, Serial No.: DNA 08070142), then diluted with 3 mL of 100% analytical grade methanol, filtered through a Polytetrafluoroethylene (PTFE) 0.22-micrometer syringe filter, and transferred into 2 mL vials for GC-MS analysis.[30]

GS-MS Method

At Jomo Kenyatta University of Agriculture and Technology (JKUAT), Kenya, a Gas Chromatography Mass Spectrometer system (Model: Shimadzu GC-MS QP-2010SE, Serial No. 02Q53497QQ5Q) was employed for GC-MS analysis. A nonpolar BPX5 column, with the following characteristics, was used: film thickness (adsorbent) of 0.25 μm, an inner diameter of 0.25 mm, and a length of 30.0 m. The programmed column oven temperature began at 55.0°C and slowly increased by 10.0°C per minute until it reached an isothermal temperature of 280.0°C with a time hold of 15.50 minutes. The temperature for the split mode of injection was programmed at 200°C, and the split mode used was in the ratio of 1:10. The flow control mode was programmed with 1.08 mL/min of carrier gas (Helium, ultra-high purity instrument grade, 99.999%), a pressure of 11.3 psi, a linear velocity of 37.8 cm/sec, 3.0 mL/min purge flow and 14.9mL/min total flow. The interface of GC-MS was programmed to a temperature of 250°C to prevent recondensation of separated analytes. The temperature of the ion source was programmed at 200 °C, and the solvent cut time was set to 2.5 min. The entire process took 35.5 minutes. The compounds' peaks at various mass-to-charge ratios were used to determine the identity of phytochemicals. The mass spectral library was employed in the determination of the unknown spectra (NIST-11).[31]

Molecular docking
Molecular docking validation

Method validation was done to enhance the accuracy, reliability, and reproducibility of molecular docking. Briefly, the native ligand and water molecules were separated from the three-dimensional (3D) x-ray protein structure and prepared for docking in the Maestro Schrodinger 2023 version. The binding pockets were identified using the site map. The mapped sites were superimposed onto the protein to determine the binding pocket for the native ligand onto the protein. The native ligand was prepared and re-docked onto the identified pocket. The native ligand was superimposed with the co-crystallized ligand to generate the root mean square deviation (RMSD). An optimal RMSD of <2 A° was considered for docking and indicated that the procedure could be subsequently used for small molecules identified by GC-MS.[32]

Protein Preparation

The *Mycobacterium tuberculosis* proteins of interest were obtained from the Protein Data Bank (PDB) database: Polyketide synthase-13 pks13 and HTH-Transcriptional regulator (EthR), with a PDB code of 3V3Y and 3Q0V, respectively. For the preparation of the protein binding site, chain A complex was employed by deleting the other chains. All the water molecules beyond 5 Å were deleted from the complex. Hydrogen atoms were added to the model using the Maestro interface (Version 13.5; Schrodinger's 2023) based on an explicit all-atom model. The final preparation of the protein's complexes was done using a multistep Schrodinger's protein preparation tool (Protein Preparation workflow), followed by energy minimization using the OPLS4 force field. Lastly, the Receptor Grid Generation was done to identify the binding pocket region.[33]

Ligand Preparation

A local library of phytochemicals identified in *A. zygia* by GC-MS was created for molecular docking evaluation. The two-dimensional structures of the compounds in the SDF format were obtained from PubChem and imported into the Maestro Schrodinger 2023 version. The OPLS4 force field was used, the neutral charge was enhanced, and the tautomer's generation was deactivated.[33]

Ligand Docking

The 3V3Y and 3Q0V binding pockets were docked with the prepared ligands. The ligands' final docking poses were rated according to their binding energy (Docking score), and a docking score of ≤ -7 kcal/mol was considered appropriate.[33] The binding affinities were compared with those of isoniazid and ethionamide, standard anti-TB drugs.

Ligand-based ADME/Toxicity Prediction

The docked compounds with docking scores ≤ -7 kcal/mol were entered as SMILES into ADMETLab 2.0 from the Computational Biology & Drug Design Group (https://admetmesh.scbdd.com/), and their properties were computed using the algorithms. ADMETLab 2.0 employed Caco2-cell (heterogeneous human epithelial colorectal adenocarcinoma cell lines) and MDCK (Madin–Darby Canine Kidney) cell models to forecast oral drug absorption, skin permeability, human intestinal absorption, and transdermal drug absorption [34]. For the drug-likeness, the Qikprop Maestro Schrödinger 2023 model was used. The ligands were obtained from PubChem in SDF format, imported into Maestro's working space, and a Qikprop prompt was run. To predict drug-likeness, the following properties were evaluated: MW: molecular weight <500; Donor HB: hydrogen bond donor 0.0–6.0; acceptor HB: hydrogen bond acceptor 2.0–20.0; SASA: total solvent accessible surface area 300.0–1000.0; QPlogPo/W: predicted octanol/water partition coefficient −2.0–6.5; QPlogBB: predicted brain/blood partition coefficient. -3.0–1.2, QPlogS; predicted aqueous solubility, log S. S in mol dm−3, −6.5–0.5, Percent Human-Oral Absorption: Predicted human oral absorption on a 0 to 100% scale (>80% is high, <25% is poor).[33]

Ethical Consideration

This work was approved by Kenya Medical Research Institute's Scientific and Ethics Research Unit (KEMRI/SERU/CTMDR/CSCP105/4540). *A. zygia* root bark was harvested with much care to enhance sustainability. Antimycobacterial assays were conducted with the help of trained personnel in a biosafety level two (BSL 2) laboratory to protect the researchers from potential infection. During the experiments, the use of PPE and adherence to SOPs were observed.

Statistical Analysis

Microsoft Excel (version 2019) was used to determine the mean, standard deviations, ANOVA (one-way), and post hoc test. Results were expressed as means and standard deviations, and their statistically significant difference was evaluated at a p-value less than 0.05.[35]

RESULTS

Percentage Extraction Yield, Cytotoxicity, Anti-mycobacterial Activity, and Antimycobacterial Synergistic Activity

In the organic solvents, methanol demonstrated the highest percentage extraction yield, 64.8 mg (6.48%), followed by dichloromethane, 42.2 mg (4.22%), ethyl acetate, 24.3 mg (2.43%), and hexane, 6.7 mg (0.67%). However, the water had an extraction yield of 81.1 mg (8.11%) (Table 1).

All the extracts exhibited cytotoxicity concentration (CC_{50}) values ≥ 80 µg/mL, with the aqueous extract demonstrating the greatest value (2997.60 µg/mL), and the dichloromethane extract presented the lowest CC_{50} (82.59 µg/mL). Rifampicin exhibited a CC_{50} of 534.49 µg/mL (39) Table 1).

Methanol and water exhibited antimycobacterial activity with MIC99 of 625 µg/mL and 2500 µg/mL, respectively (Table 1), However, hexane, DCM, and ethyl acetate were inactive against *Mycobacterium smegmatis (Msm)*.

Table 2 delineates the effects of the combination of rifampicin with the methanolic (Extract 1) and aqueous (Extract 2) extracts of *A. zygia* root bark. The MIC_{99} of RIF was decreased by 32 and 8-fold with Fractional Inhibitory Concentration (FIC) values of 0.03 and 0.13 for the methanolic and aqueous extracts, respectively. The MIC_{99} of the RIF singly was 12.50±0 µg/mL, while 0.39±0 µg/mL and 1.56±0 µg/mL when combined with methanolic and aqueous extracts, respectively (Table 2).

Phytochemical Profiling and Characterization

The extractable classes of phytochemicals detected in both aqueous and methanolic extracts were alkaloids, flavonoids, tannins, and phenols, while terpenoids were only present in aqueous extracts; however, saponins were absent in both extracts. The GC-MS analysis of aqueous and methanolic extracts revealed the presence of 21 phytochemicals in each (Figure 1). In the aqueous extract, the major abundant phytochemicals detected were 4-o-methyl mannose (65.85%), beta-d-mannofuranoside methyl (18.68%), heptanoic acid 6-oxo- (2.41%), 4H-pyran-4-one, 2,3-dihydro-3,5-dihydroxy-6-methyl- (5.8%) and glycerin (1.4%) while others were less than 1% (Supplementary table 1) The major abundant phytochemicals in the methanolic extract of *A. zygia* root bark were: alpha.-d-6,3-furanose, methyl-.beta.-d-glucohexodialdo-1,4-furanoside (75.34%); 2-hexadecyl-5-methylpyrrolidine (7.6%); 1,3-propanediol, 2-(hydroxymethyl)-2-nitro- (2.8%) and 4H-pyran-4-one, 2,3-dihydro-3,5-dihydroxy-6-methyl (2.59%), while others had their abundance less than 2% (Supplementary tables 1 and 2).

In silico Studies
Validation of Molecular Docking

Root mean square deviation (RMSD) values of 0.9312 Å and 0.9773 Å for 3Q0V and 5V3Y, respectively, were obtained upon re-docking of the native ligand onto the molecular targets' binding sites. Reproducibility and accuracy of the method were demonstrated by RSMD of less than <2 A° as indicated in figures 2 and 3.

Molecular Docking

Table 3 presents the binding affinities (docking scores) of molecules displaying docking scores ≤ –7.0 kcal/mol, thus indicating strong binding potential. With a docking score of –8.945 kcal/mol, quinoline, 7-ethyl-, was the top-ranked compound against the enoyl-acyl carrier protein reductase (InhA) target (PDB ID: 3Q0V), followed by diphenyl sulfone (–8.742 kcal/mol), and ethionamide, a known anti-TB medicine (–8.803 kcal/mol). Another reference medicine, isoniazid, had a docking score of –7.366 kcal/mol. Also showing good docking scores of –7.774 and –7.247 kcal/mol, respectively, were 4H-Pyran-4-one, 2,3-dihydro-3,5-dihydroxy-6-methyl, and 2,4-di-tert-butylphenol. 7-ethyl-quinoline, again displayed the best docking score (–7.644 kcal/mol), followed by diphenyl sulfone (–7.433 kcal/mol) and ethionamide (–7.069 kcal/mol), against Polyketide Synthase-13 (Pks13) (PDB ID: 3V3Y). With Pks13, isoniazid displayed a rather weaker interaction (–5.894 kcal/mol).

Absorption, Distribution, Metabolism, Excretion, and Toxicity (ADME/T)

Table 4 displays the ADMET and drug-like characteristics of ten compounds having docking scores ≤ -7 kcal/mol. Eight compounds (1, 2, 3, 5, 6, 7, 8, and 10) showed high human intestinal absorption properties, while compounds 4 and 9 showed low absorption. Log S, or water solubility, values ranged from -6.43 (compound 7) to -0.098 (compound 4). None of the compounds behaved as P-glycoprotein substrates; all showed $CaCO_2$ permeability values between -5.282 and -4.352 cm/s. P-glycoprotein inhibitory activity was shown only by compound 9. Plasma protein binding varied greatly, according to distribution analysis, from 0.321% (compound 5) to 96.53% (compound 2). Six compounds, 1, 2, 3, 5, 6, and 8, showcased blood-brain barrier permeability; volume of distribution values ranged from 0.409 L/kg (compound 5) to 4.896 L/kg (compound 9). The metabolic profile revealed different CYP enzyme interactions over the series of compounds. Compounds 1, 6, 8, and 9 saw CYP1A2 inhibition; compounds 1, 2, 8, 9, and 10 were CYP1A2 substrates. The compounds 1, 2, and 9 demonstrated limited CYP2C19 inhibitory activity. Elimination values for total clearance ranged from 0.501 mL/min/kg (compound 2) to 15.23 mL/min/kg (compound 10). With most exceeding the allowed threshold of 0.3, half-life predictions ranged from 0.054 (compound 7) to 0.817 (compound 6). Compounds 2, 3, 6, and 10 showed carcinogenic potential according to toxicity assessment; compounds 1 and 4 had positive AMES toxicity. No compound demonstrated hepatotoxicity or hERG blocking action. Compounds 1, 3, 6, 7, 9, and 10 had skin sensitization potential; compounds 1 and 9 were predicted to be respiratory toxic. With molecular weights ranging from 126.2 g/mol to 337.5 g/mol, all compounds satisfy Lipinski's Rule of Five; only compound 7 shows one violation because of its high Log *P* value of 8.263.

TABLE 1: Extraction yield, Cytotoxicity, and Anti-mycobacterial Activity

Extract/Drug	% Yield	Cytotoxicity (CC50 in µg/mL)	Antimycobacterial Activity (MIC99 in µg/mL)
Hexane	0.67	1409.62±0.0	NA
Dichloromethane	6.22	82.59±0.0	NA
Ethyl acetate	2.43	1580.54±0.0	NA
Methanol	6.48	1295.01±0.0	625±0.0b
Water	8.11	2997.60±0.0	2500±0.0b
Rifampicin	-	534.49±0.0	15.63±0.0b

Cytotoxicity concentration (CC50), Not active (NA), *P* value < .05 (b)

TABLE 2: Drug Combination Study of Rifampicin and Bioactive Extracts

Drug/Extract	MIC99 (µg/mL), singly	MIC99 (µg/mL), in combination	MIC99 fold reduction factor	FIC	FICI
Extract 1	625±0	312.25±0	2	0.50	0.50
Rifampicin	12.50±0	0.39±0	32	0.03	
Extract 2	2500±0	1250±0	2	0.50	0.63
Rifampicin	12.50±0	1.56±0	8	0.13	

Extracts 1 and 2 are methanolic and aqueous extracts of A. zygia root bark, respectively. FIC: Fractional Inhibitory Concentration and FICI: Fractional Inhibitory Concentration Index. MIC99; Minimum Inhibitory Concentration.

**FIGURE 1: Figure A; chromatogram of aqueous while Figure B; methanolic extract chromatogram of A. zygia root bark**

Figure; A   Figure; B
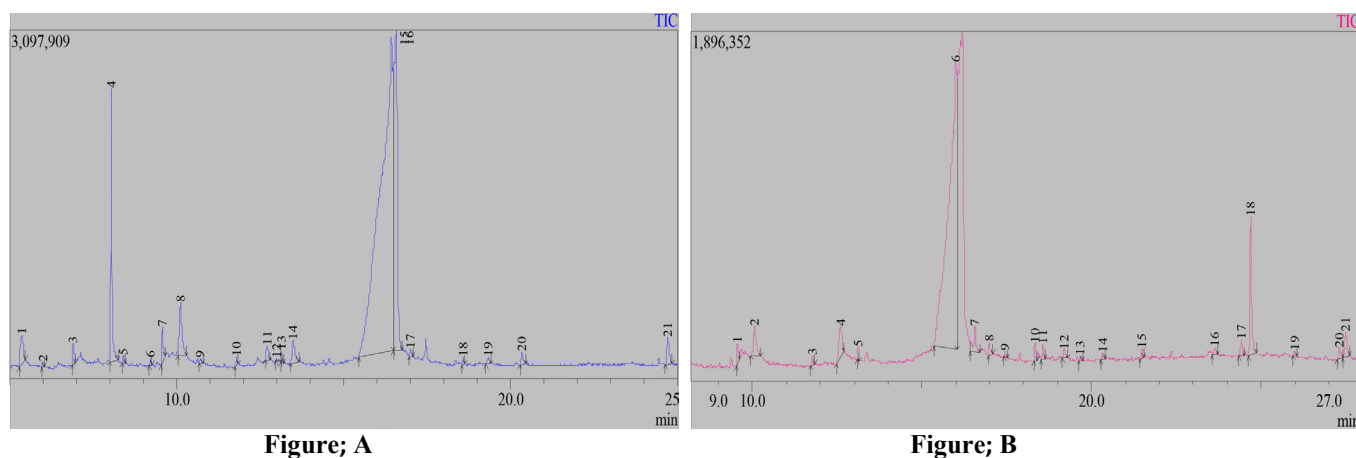
**FIGURE 2:** The Pose for Co-crystalized Ligand in the Binding Site of 3Q0V before Redocking
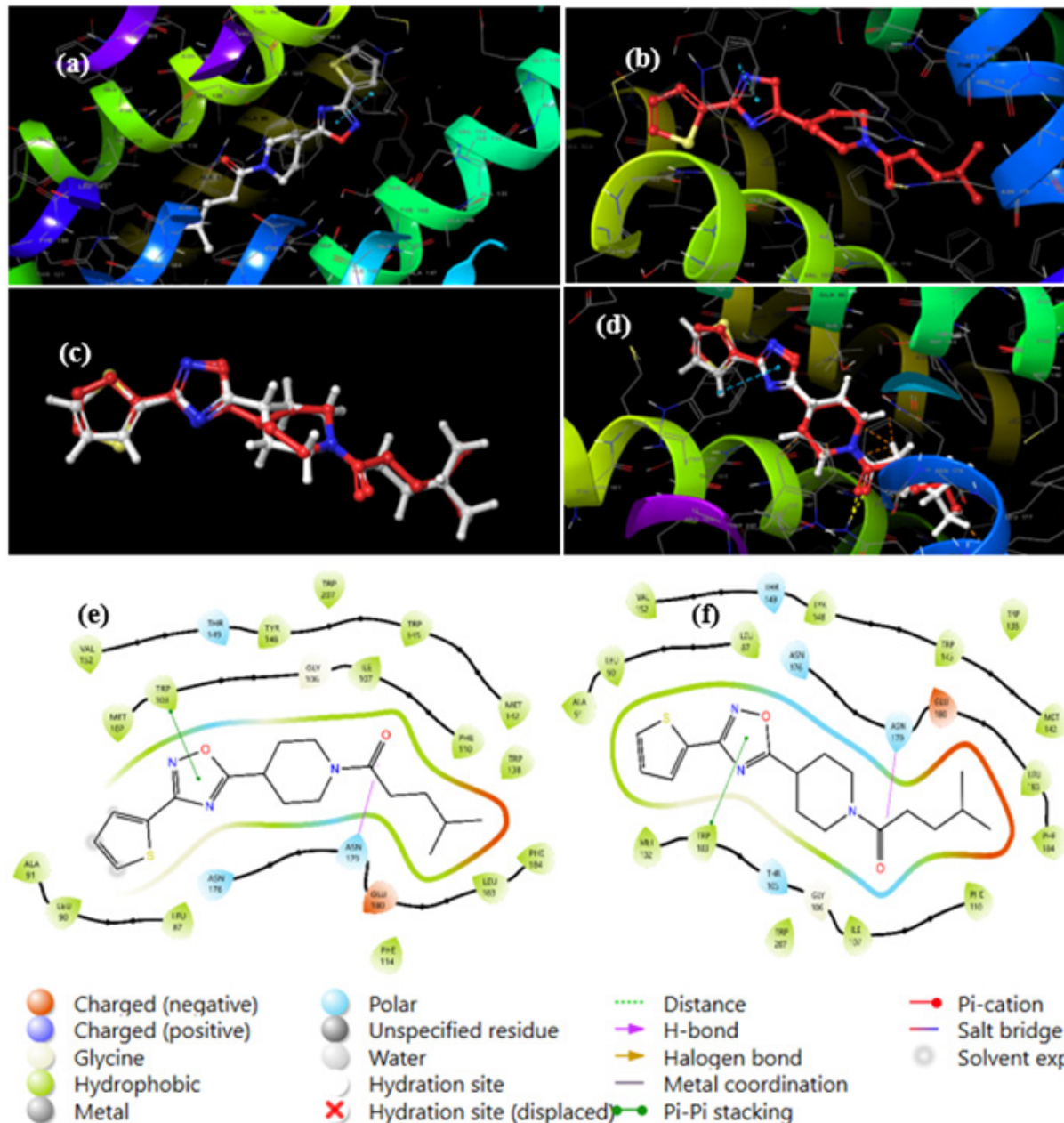
(a), the pose of co-crystalized ligand (red) in the binding site after re-docking (b), the pose of native ligand before and after redocking white and red, respectively (c), and the pose of superposed ligand on the native ligand in the protein before and after redocking white and red, respectively (d). Two-dimensional interactions of co-crystalized ligand in the binding site of enoyl-acyl carrier protein reductase before redocking (e). The interactions of the re-docked co-crystalized ligand with amino acid residues in the binding site of enoyl-acyl carrier protein reductase (f).

FIGURE 3: Maps of the Pose for Co-Crystalized Ligand in The Binding Site of Polyketide Synthase
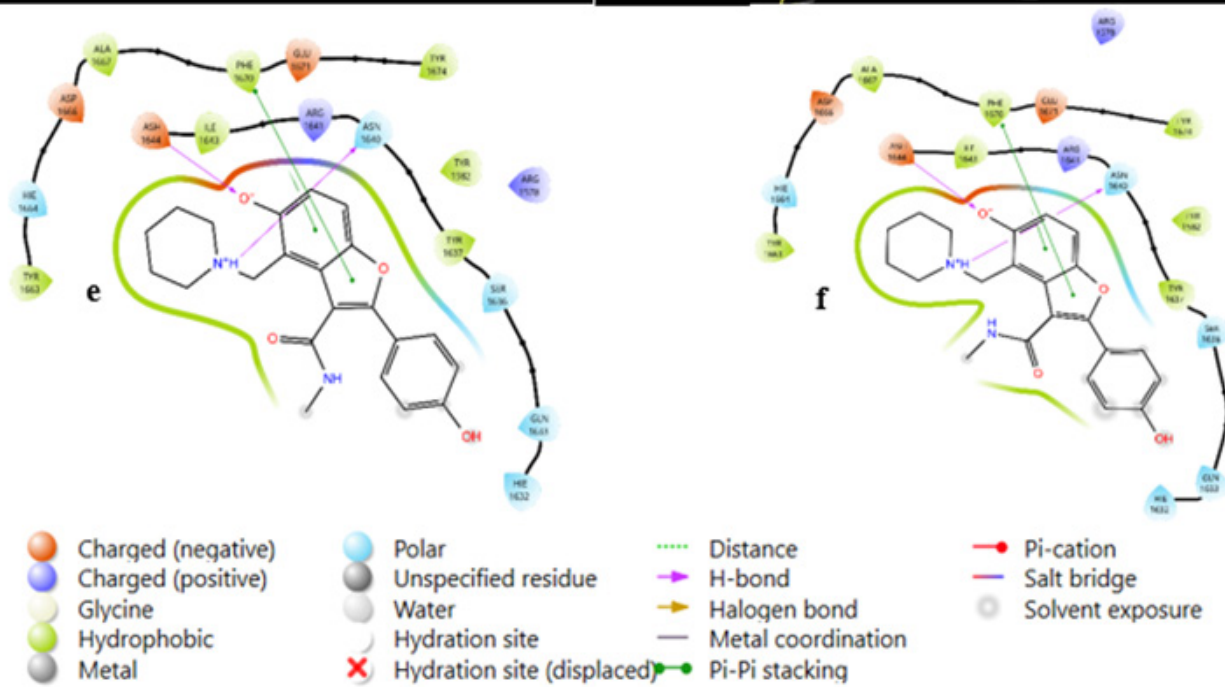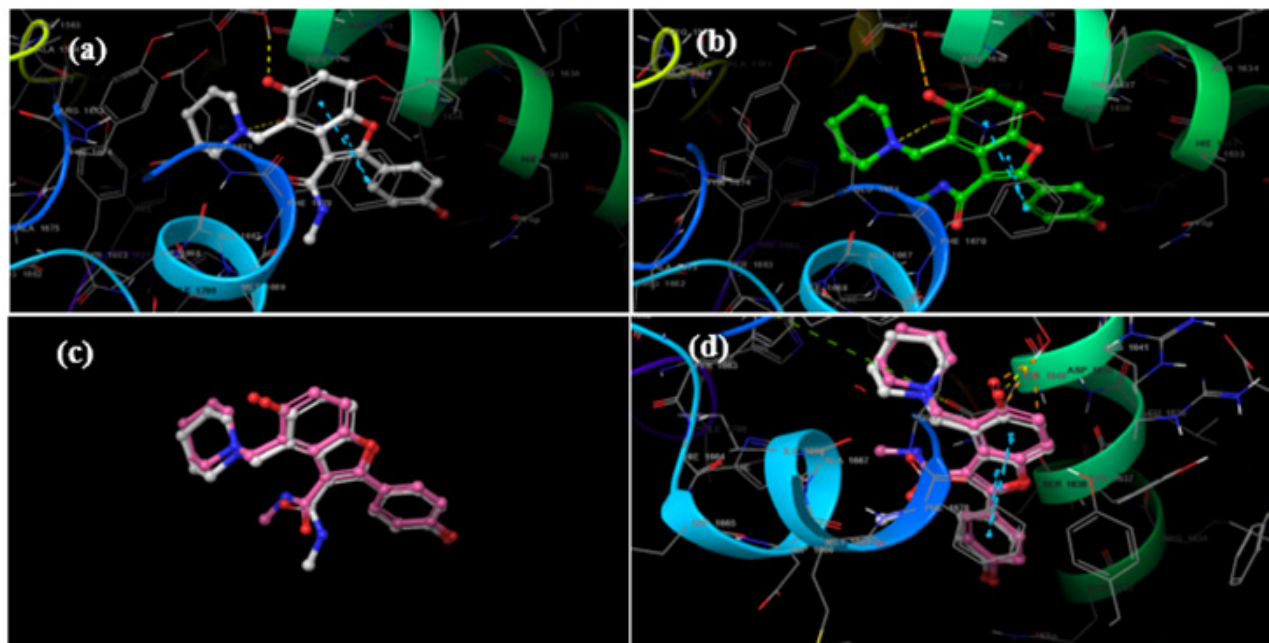
(a), the re-docked pose of co-crystalized ligand (green colour) (b), the pose of native ligand before and after redocking white and pink, respectively (c), and the pose of superposed ligand on the native ligand in the protein before and after redocking white and pink, respectively (d). Two-dimensional interactions of co-crystalized ligand in the binding site of polyketide synthase in (e). The interactions of the re-docked co-crystalized ligand with amino acid residues in the binding site of polyketide synthase (f)

FIGURE 4: Phytochemicals with Strong Binding Affinities, A Docking Score of <-7
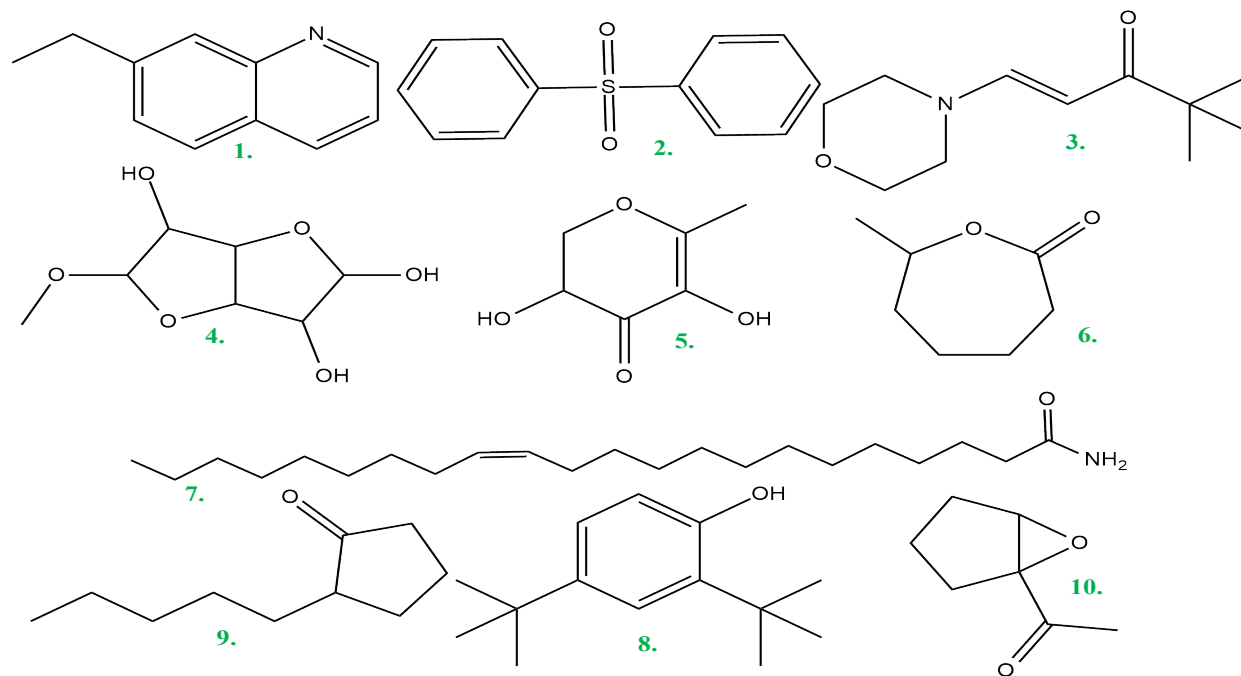
TABLE 3: Compounds Demonstrated Binding Affinities of Docking Score < -7 Kcal/Mol

Compound	Docking Score
The enoyl-acyl carrier protein reductase (InhA) PDB code 3Q0V	
Quinoline, 7-ethyl-	-8.945
Diphenyl sulfone	-8.742
Pent-1-en-3-one,4,4-dimethyl-1-(4-morpholino)-	-7.966
Alpha.-d-6,3-Furanose, methyl-.beta.-d-glucohexodialdo-1,4-furanoside	-7.897
4H-Pyran-4-one, 2,3-dihydro-3,5-dihydroxy-6-methyl	-7.774
2-Oxepanone, 7-methyl	-7.654
Erucylamide	-7.591
2-Pentyl cyclopentanone	-7.476
2,4-Di-tert-butylphenol	-7.247
Cyclopentane, 1-acetyl-1,2-epoxy-	-7.205
Isoniazid	-7.366
Ethionamide	-8.803
Polyketide synthase-13 pks13 PDB code 3V3Y Compound	
Quinoline, 7-ethyl-	-7.644
Diphenyl sulfone	-7.433
Isoniazid	-5.894
Ethionamide	-7.069

TABLE 4: Descriptors of Absorption, Distribution, Metabolism, Elimination, and Toxicity ADMET of Docked compounds with a d-score of >-7 kcal/mol

Properties	1	2	3	4	5	6	7	8	9	10	Acceptable values
Absorption											
Log S	-2.769	-3.49	-1.026	-0.098	-0.67	-1.74	-6.43	-2.52	-4.6	-0.84	-2 to -4
HIA	High	High	High	Low	High	High	High	High	Low	High	High
Log P in (cm/s)	-4.352	-4.663	-4.42	-5.282	-4.85	-4.44	-4.89	-4.46	-5.05	-4.46	>-5.15
P-gp substrate	No	No	No	No	No	No	No	No	No	No	No
P-gp I inhibitor	No	No	No	No	No	No	No	No	Yes	No	No
Log Kp	-5.2	-5.93	-6.55	-8.98	-7.44	-6.14	-1.86	-5.15	-3.87	-6.81	<-5.0
F20%	Low	High	High	High	High	High	High	Low	Low	High	High
F30%	Low	High	High	Low	High	Low	Low	Low	low	High	High
Distribution											
PPB (%)	86.33%	96.53%	21.77%	10.57%	0.321	0.608	0.983	0.92	0.984	0.335	<90
BBB permeability	Yes	Yes	Yes	No	Yes	Yes	No	Yes	No	No	No
VD in (L/kg)	1.477	0.701	1.229	0.529	0.409	0.709	2.39	1.123	4.896	1.178	0.04–20
FU in plasma (%)	11.37%	3.72%	77.43%	86.35%	0.679	0.485	0.012	0.063	0.05	0.697	>5
Metabolism											
CYP1A2 inhibitor	Yes	No	No	No	No	Yes	No	Yes	Yes	No	No
CYP1A2 substrate	Yes	Yes	No	No	No	No	No	Yes	Yes	Yes	No
CYP2C19 inhibitor	Yes	Yes	No	No	No	No	No	Yes	Yes	Yes	No
CYP2C19 substrate	No	Yes	Yes	Yes	No	No	No	No	Yes	Yes	No
CYP2C9 inhibitor	No	Yes	No	No	No	No	No	No	Yes	No	No
CYP2C9 substrate	Yes	No	No	No	No	Yes	Yes	No	Yes	No	No
CYP2D6 inhibitor	Yes	No	No	No	No	No	No	Yes	Yes	Yes	No
CYP2D6 substrate	Yes	No	No	No	No	No	No	No	Yes	Yes	No
CYP3A4 inhibitor	No	No	No	No	No	No	No	No	No	No	No
CYP3A4 substrate	No	Yes	Yes	No	No	No	No	No	Yes	No	No
Elimination											
TC (mL/min/kg)	5.043	0.501	6.088	1.567	2.05	9.944	4.487	9.213	6.3	15.23	>5
Half-life < 3hrs	0.344	0.122	0.787	0.533	0.748	0.817	0.054	0.809	0.324	0.789	<0.3
Toxicity											
Carcinogenicity	No	Yes	Yes	No	No	Yes	No	No	No	Yes	No
AMES toxicity	Yes	No	No	Yes	Yes	No	No	No	No	No	No
hERG blockers	No	No	No	No	No	No	No	No	No	No	No
Hepatotoxicity	No	No	No	No	No	No	No	No	No	No	No
Skin sensitization	Yes	No	Yes	No	No	Yes	Yes	No	Yes	Yes	No
Respiratory Toxicity	Yes	No	No	No	No	No	No	No	Yes	No	No
Rat Oral Toxicity	No	Yes	No	No	No	No	No	No	No	No	No
Physicochemical properties (Lipinski Rule #Violations)	Yes; 0	Yes; 0	Yes; 0	Yes; 0	Yes; 0	Yes; 0	Yes; 1	Yes; 0	Yes; 0	Yes; 0	
H-bond donors	0	0	0	3	2	0	1	0	1	0	≤ 5
H bond acceptors	1	2	2	6	4	2	1	1	2	2	≤ 10
MW (g/mol)	157.2	218.2	197.2	192.1	144.1	128.2	337.5	154.3	206.3	126.2	≤ 500
Log P O/W	3.074	2.554	1.184	-1.933	-0.53	1.678	8.263	2.921	4.832	0.413	≤ 5

Log P; CaCO2 permeability, Log Kp; skin permeation, HIA; Human Intestinal Absorption, hERG blockers; Cardiovascular toxicity, The Log P O/W; logarithm of the octanol/water distribution coefficient, Log S; water solubility, VD; Volume Distribution, FU; Fraction unbound, BBB; Blood Brain Barrier.

FIGURE 5: The interaction of Polyketide Synthase-13 and Enoyl-Acyl Carrier Protein Reductase (InhA) with A. zygia Compounds
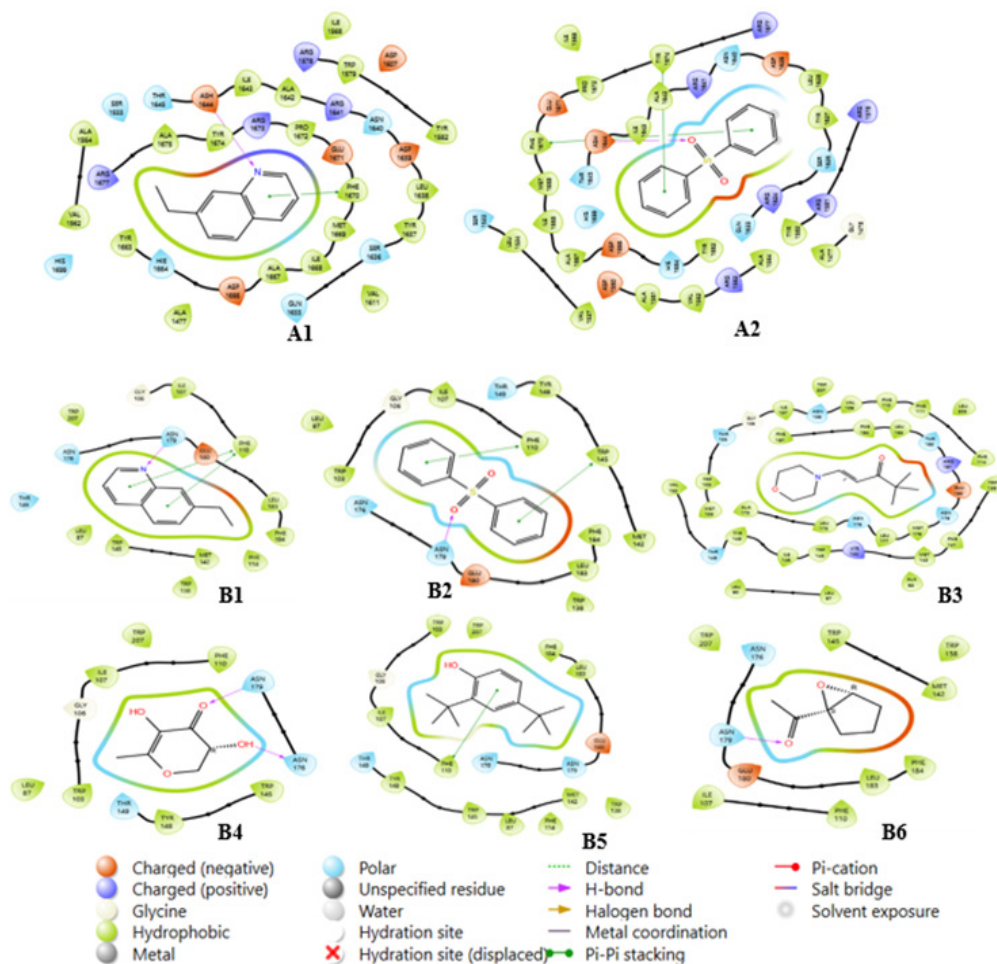
A1 and A2 indicate the top compounds interaction with Polyketide synthase-13 pks13 (PDB code 3V3Y) while Figure B1, B2, B3, B4, B5 and B6 top compounds interaction with The enoyl-acyl carrier protein reductase (InhA) (PDB code 3Q0V)

DISCUSSION
Percentage Extraction Yield, Cytotoxicity, Anti-mycobacterial Activity, and Antimycobacterial Synergistic Activity
The current study is in agreement with the extraction carried out on the stem barks of *A. coriaria*, whereby methanol and acetone (polar and semipolar solvents) showed the highest extractable phytochemicals, 23.2%, and 23.0%, respectively [36]. In addition, the extractability of these solvents is consistent with Mmushi's (2010) findings, which showed that methanol was the most effective solvent and hexane extracted the fewest phytochemicals.[37]

The National Cancer Institute classifies the cytotoxicity of plant extracts as CC50<20 µg/mL being highly cytotoxic, CC_{50} of 21 to 200 µg/mL being moderately cytotoxic,

CC_{50} of 201 to 500µg/mL being weakly cytotoxic, and CC_{50} >500 µg/mL being noncytotoxic [38]. In this study, the cytotoxicity of the extracts ranged from 42.00 µg/mL (moderately cytotoxic) to >500 µg/mL (no cytotoxicity) on the monkey Vero cells. The extracts of *A. zygia* root barks exhibited significantly low cytotoxicity (no cytotoxicity) with CC_{50} >500 µg/mL, except the DCM extract, which exhibited moderate cytotoxicity (CC_{50} <100 µg/mL) (Table 1). The cytotoxicity results for *A. zygia* root bark indicate that the extracts are within acceptable cytotoxicity levels against monkey Vero cells passage 17. This suggests that the root bark extracts of *A. zygia* (hexane, EtOAc, MeOH, and H_2O) have no appreciable intrinsic toxic phytochemicals with the capacity to kill mammalian cells at normal concentrations, except the DCM extract, which contains moderately toxic phytochemicals.

In line with the present study, a previous investigation on the Nigerian medicinal plant for the sub-acute toxicity of the aqueous extracts of *A. zygia* stem barks in mice and rats at a dosage of 5000mg/kg daily for 42 days revealed no appreciable toxicity.[39] In addition, the research conducted on the plants growing in Cameroon showed that methanolic extract of *A. zygia* demonstrated no significant cytotoxic activity on rat skeletal muscles myoblast (L-6 cells) in comparison to anti-plasmodial activity against the K1 strain of *Plasmodium falciparum* and anti-trypanosomal activity against *Trypanosoma brucei rhodesiense* with selectivity indices (S.I.) of 4.5 and 22.5, respectively.[40] In contrast, *A. zygia* root bark from the Botanical Garden of the University of Ghana exhibited CC_{50} values for aqueous and hydroethanolic extracts to be 3.09 µg/mL and 3.37 µg/mL, respectively, while dichloromethane, ethyl acetate, and petroleum ether fractions exhibited CC_{50} values of 91.4 µg/mL, >100 µg/mL, and >100 µg/mL, respectively against Jurkat cell lines [41]. The discrepancy might be attributable to the use of a different cell line in the later research, the method of extraction, and the fact that the plant materials were collected from a different geographical region, both of which could have influenced the composition and quantity of extractable compounds.[36]

The antimycobacterial activity of the methanol and aqueous extracts suggests that chemicals with moderate to high polarity impede the growth of mycobacterial species. The hexane, DCM, and EtOAc extracts were inactive since these solvents extract predominantly nonpolar phytochemicals and a few polar compounds. In addition, it has been reported that nonpolar extractable phytochemicals are generally inactive against several pathogens, such as Mycobacterium species [42]. The significant antimycobacterial activity of the methanol extract compared to the aqueous extract could be due to the methanol extract's greater variety of phytochemicals, which ranged from polar to semi-polar, as opposed to the aqueous extract's predominantly polar extractable phytochemicals. The current study is consistent with previous research that evaluated the antimycobacterial activity of the stem bark of *Albizia coriaria* Welw ex and found that methanolic and acetone extracts were active against *Mycobacterium tuberculosis* and *Msm*, whereas hexane and chloroform extracts were inactive.[36] In addition, methanolic extracts of *A. zygia* stem barks demonstrated appreciable antimicrobial activity against various pathogens.[15] Based on the available literature, the current study is the first to report *in vitro* antimycobacterial activity of *A. zygia*. Although other Albizia species, such as *A. coriaria* and *A. gummifera A. adianthifolia* have been reported to have antimycobacterial properties [36,43,44]. The reference standard drug RIF showed better activity compared to the active plant extract against *Msm*. It is probable that the crude form of the plant extract accounts for the reduced mycobacterial activity of the extracts. Due to the crude nature of the extracts, matrix interferences may arise, which decrease the actual quantity of active phytochemicals at the target site, therefore diminishing the intended activity. Therefore, several phytochemicals in the matrix herbal extract might have an antagonistic effect, which reduces the crude extract's antimycobacterial effectiveness.[45]

In regards to the standard definition, a synergistic effect exists when the FICI≤0.5, an antagonistic relationship when FICI≥4, and 0.5<FICI<4 shows additive interaction.[46,47] In general, *A. zygia* root extracts displayed enhanced effectiveness of RIF against *Msm*. Methanolic and aqueous extracts demonstrated synergistic and additive interaction with the FICI of 0.5 and 0.63, respectively. This could be attributed to the extracts being from the same plant part, extracted with the solvent of close polarity index, and hence might contain slightly different phytochemicals [48]. The current study is in line with the other research conducted on selected medicinal plants, which demonstrated enhancement of the antimycobacterial activity of ethambutol and isoniazid (INH). In line with this study, the extracts of *Boswellia serrata*, *Lavandula stoechas*, and *Thymus vulgaris* exhibited synergistic interaction with FICI values of 0.125, 0.5, and 0.166, respectively.[49] It is possible that the *A. zygia* extracts could be employed to boost the antimycobacterial activity of anti-TB medicines against multidrug-resistant *Mtb*.

Phytochemical Profiling and Characterization

To identify probable phytochemicals that could be responsible for the antimycobacterial activity of *A. zygia*, phytochemical profiling and characterization were done. Alkaloids, flavonoids, tannins, phenols, terpenoids, and saponins detected in the aqueous and methanolic extracts have been reported to exhibit antimicrobial activity, including antimycobacterial, antibacterial, and antifungal activity. Similar or some of the phytochemicals revealed in this study were also found in the stem bark and volatile oil of *A. zygia* [17,50] and in the root bark of *A. coriaria* (a plant belonging to the same genus).[36]

Various phytochemicals detected by GC-MS have important therapeutic uses in the treatment of numerous diseases in both humans and animals. 4H-Pyran-4-one, 2,3-dihydro-3,5-dihydroxy-6-methyl- (5.8%) is reportedly to exhibit antioxidant activity [51]. The 2,4-di-tert-butylphenol (0.19%) and its analogous exhibit antibacterial activity against multidrug-resistant bacteria such as *Pseudomonas aeruginosa* and *Staphylococcus aureus*, antioxidant, antifungal, antiviral, insecticidal, and nematocidal activity [52]. Morpholine and its analogues exhibited antibacterial activity against *E. coli* (MIC = 1.91 mg/mL).[53] Diphenyl sulfones exhibit antibacterial and anticancer activity [54]. Mono and multi-substituted quinolines exhibited antifungal activity and were bioactive against both gram-positive and gram-negative bacteria [55] as well as antimycobacterial activity against *Mtb* H37Rv (ATCC 27294) with an MIC of 6.25 µg/mL [56]. Hydroquinone isolated from Artemisia *capillaris* exhibited antimycobacterial activity against MDR *Mtb* strains (MIC=12.5 µg/ml) [57]. Antimicrobial property against *S. aureus* and *P. fluorescens* was demonstrated by succinic acid extracted from *Brassica juncea Coss* Var. foliosa Bailey with MICs of 2.0 and 2.5 µg/mL, respectively. [58]. Hexadecanoic acids have been reported to possess numerous antimicrobial activities such as antibacterial and antioxidant activity, nematicide, anti-androgenic, and hypocholesterolemia [59]. GC-MS analysis of the active acetone and methanolic extracts of *A. coriaria* against *Msm* and *Mtb* revealed the presence of hexadecanoic acid and hydroquinone, which is consistent with the current study [36]. Therefore, the antimycobacterial activity may

be attributed to identified phytochemicals reported to inhibit *Mtb* strains and other bacteria.

In silico studies
Molecular Docking
Molecular docking provides information on the binding affinities and interactions between compounds and target proteins. This technique is essential for identifying and developing new drugs or potential drug candidates before they go through costly and drawn-out trial validation. The reference drugs ethionamide and isoniazid were docked to the target proteins to confirm the docking approach and provide a standard for comparison with the phytochemicals from *A. zygia*. Of 42 GC-MS-identified phytochemicals in both aqueous and methanolic extracts, ten exhibited significant binding affinities with a docking score of >-7 kcal/mol (Figure 4 and Table 3).

Mycobacterium tuberculosis (Mtb) polyketide synthase-13 (pks-13) is a required enzyme that plays the role of the mycolic acid synthetic step in mycolic cell walls. In *Mtb*, mycolic acid is involved in the virulence and drug resistance of the Mycobacterium. pks-13 is involved in the last step of the assembly of the mycolic acids. The enzyme catalyzes the linking of two fatty acyl chains, a step that is necessary for the synthesis of mycolic acid. pks-13 is a multifunctional enzyme that has domains such as keto-synthase, acyltransferase, and acyl carrier protein. The inter- and intra-arrangements of these domains play a vital role in the enzymatic function of the protein.[60] The mycolic acids produced by pks-13 provide additional input to the strength and the resistance of the mycobacterial cell wall, which enables *Mtb* to live in unfavorable conditions: within a host macrophage.[60] Therefore, pks-13 is regarded as an essential target for the new anti-tuberculosis agents since it plays a crucial part in the formation of mycolic acids and, consequently, the existence of *Mtb*. If there are inhibitors to pks-13, they may prevent the synthesis of the cell wall and increase the effectiveness of the presently available drugs and novel anti-tuberculosis compound development. The identified phytochemicals interacted with various amino acid residues of the pks-13 protein.[60] The Quinoline, 7-ethyl- exhibited π-π and hydrogen bonding interactions with Phe1670 and Ash1644 residues, respectively (Figure 5). Diphenyl sulfone exhibited π-π and hydrogen bonding interactions with Phe1670, Tyr1673, and Ash1644 aromatic amino acid residues, respectively. In line with this study, Katharigatta, et al 2021, the type of interaction exhibited between the compounds and amino acid residues of pks-13 protein was π-π interaction for Phe1590, Tyr1637, Phe1585, Tyr1674, Phe1670, and His1699, and hydrogen bonding for Ser1636 and Asn1640 [60]. Therefore, the mechanism of action of *A. zygia* against *Mycobacterium smegmatis* could be attributed to the compounds 7-ethyl-quinoline and diphenyl sulfone, which demonstrated inhibition (≥-7 kcal/mol) of the pks-13 protein responsible for the multidrug resistance of *Mycobacterium tuberculosis*.

HTH (helix-turn-helix) transcriptional regulators are proteins that play a crucial role in gene expression by binding to specific DNA sequences and influencing the transcription of target genes[61]. One such regulator is EthR, a protein found in *Mtb*. EthR is a transcriptional regulator involved in bacterial resistance to the antibiotic ethionamide. Ethionamide is used in the treatment of tuberculosis (TB), particularly multidrug-resistant TB (MDR-TB).[62 63] EthR regulates the expression of EthA, a monooxygenase enzyme that activates ethionamide by converting it to its active form. EthR contains a helix-turn-helix motif, which allows it to bind to specific DNA sequences in the promoter region of the EthA gene. When EthR binds to the EthA promoter, it represses the transcription of the EthA gene, leading to reduced production of the EthA enzyme. This results in decreased activation of ethionamide, contributing to bacterial resistance. Because EthR represses EthA and reduces the effectiveness of ethionamide, it has become a target for developing inhibitors that can enhance the activation of ethionamide. By inhibiting EthR, the repression of EthA is lifted, leading to increased activation of ethionamide and improved treatment efficacy.[62]

The ten phytochemicals exhibited desirable binding affinity with EthR proteins, demonstrating two types of interaction. The π-π interaction was exhibited in the phenyl groups of the identified phytochemicals with Phe110 and Trp145 residues. Moreover, the hydrogen bonding was exhibited on keto, amine, amide, and hydroxyl functional groups with Ans179, Ans176, Gly106, and Glu156 amino acid residues. All the compounds that demonstrated significant binding affinity had at least a phenyl or alkyl chain and a heteroatom such as N or O. In line with this study, most compounds docked onto the EthR protein, demonstrated hydrogen bonding interaction with Ans179 and Ans176 residues, and π-π stacking interactions with Phe110, Trp207, and Trp103 amino acid residues [63]. The ten identified phytochemicals (Table 3) demonstrated significant binding affinity to EthR, suggesting that they can inhibit its repressor activity. The identified inhibitors may have the potential to restore the sensitivity of *Mtb* to ethionamide, making them valuable adjuncts in TB treatment. Therefore, the EthR inhibitors identified may be developed as co-therapeutics with ethionamide to combat MDR-TB.

Absorption, Distribution, Metabolism, Excretion, and Toxicity (ADME/T)
The compounds were characterized as having mild to moderate lipophilicity and good absorption, a prerequisite for any drug that is given orally. The log S values of the compounds ranged between -2. 769 to -4. 6, which is close to Lipinski's acceptable range of -2 to -4. Therefore, demonstrating good water solubility except for Compound 7 with a log S of -6. 43. The results on Human Intestinal Absorption (HIA) reveal that the value is high for most of the compounds, which indicates good permeability based on Log P values; nonetheless, compounds 4 and 9 had lower HIA, and formulation modification might be needed. The PPB varies with drugs' values to be less than 90% for most compounds, indicating an adequate amount of free drug to exert the therapeutic effect [64]. All the compounds demonstrated no interaction with P-glycoprotein substrate (P-gp), indicating no probability of drug efflux from tissues and organs, thus decreasing bioavailability. The inhibitory activity of Compound 9 on P-gp I, suggests an interference with the pharmacokinetics of other co-administered drugs.[65]

Five of the ten compounds, 1, 2, 3, 5, 6, and 8 showed a probability of penetrating the blood-brain barrier (BBB), therefore, any of the drugs developed under this scaffold has the chance of affecting the CNS, although this might be desirable for CNS drugs, it also poses a major drawback of having off-target CNS effects [66] The compounds demonstrated acceptable volume distribution (VD), and several studies show that VD values reveal extensive tissue distribution, further implying systemic availability of the respective drugs.[64,66]

The elimination evaluation of the docked compounds reveals the clearance values (0.501-15.23 mL/min/kg) and the half-life values (0.054-0.817 hours), which point towards a rapid elimination. Clearance compounds (for instance, compounds 6, 8, 9, and 10) may need more often dosing or a modified-release product to achieve therapeutic concentration. The fast rate of elimination reduces the potential toxicity and accumulation of the drugs. Nevertheless, even the compounds that demonstrate rates of clearance and half-life amounts as low as compounds 2 and 7 prove that it is crucial to introduce new strategies for formulations to provide effectiveness. This has the effect of requiring optimization of the dosing regimens and the delivery systems to ensure the efficacy of the drugs, and at the same time, compliance by the patients [66]. Therefore, more in vivo studies may be required to establish these results and enhance the pharmacokinetics.

The metabolism profiles of the docked compounds reveal significant interactions with various cytochrome P450 (CYP) enzymes, which are critical for drug metabolism.[67] Some of them interact either as inhibitors or as substrates, conforming with Waring (2020), that CYP1A2 is involved in the metabolism of xenobiotics and that there is potential for drug-drug interactions.[67] Of the compounds, 1, 2, 8, and 9 were found to be potent inhibitors of CYP2C19, and the others are substrates for the enzyme. This is comparable to Durán-Iturbide (2020), regarding the enzyme's relevance to clinical practice in metabolizing PPIs and antiplatelet medications. Compounds 2, 6, and 9 may affect the CYP2C9 metabolized drugs as warfarin. Unlike CYP3A4, regarded as being involved in the metabolism of several drugs and substances, interaction with it is low and observed only in the case of Compound 2.[64,66]

The compounds in question demonstrated variable toxicity. The carcinogenic effect was exhibited in compounds 2, 3, and 6, while the other are non-carcinogenic. The test reveals mutagenicity in compounds 1, 4, and 5. None of the compounds interact with hERG, which implies a small risk of cardiac arrhythmia. All compounds under investigation demonstrated no hepatotoxicity; therefore, a low risk of liver damage is expected. Skin sensitization was exhibited in compounds 1, 3, 6, 7, 9, and 10, while respiratory toxicity was acknowledged for compounds 1 and 9; thus, desirable formulation and administration strategies must be employed. No compounds exhibit rat oral toxicity, therefore, the acute toxicity threat is low.[66] Additionally, these findings point to the need for subsequent *in vitro* and *in vivo* experiments for the confirmation of safety and minimization of the effects of the identified risks while synchronizing with the guidelines for drug development.

CONCLUSIONS

A. zygia phytochemicals possess antimycobacterial activity and synergistic interaction with an anti-TB drug (rifampicin) and are not toxic to mammalian cells. Molecular docking pointed to high binding of 7-ethyl-quinoline, 2,4-di-tert-butylphenol, and diphenyl sulfone to targets on *Mtb*; the findings supported the potential of co-therapeutics with ethionamide. The compounds possess good oral absorption with low P-gp interaction and acceptable distribution. However, the short terminal half-life, the possibility of cross-CNS effects, and CYP enzyme interaction require consideration. Subsequent *in vivo* investigations and formulation are needed to achieve optimal therapeutic effects, reduce potential side effects, and confirm these initial observations. The findings justify the ethnomedical utilization of the *A. zygia* plants in treating TB in Kenya. However, further *in vitro* and *in vivo* studies are required to be performed on individual compounds for validation.

REFERENCES

1. Zhang Y, Huang J, Du L. The top-cited systematic reviews/meta-analyses in tuberculosis research. Medicine. 2017;96(6):e4822. doi:10.1097/md.0000000000004822

2. Liu Y, Wang J, Wu C. Microbiota and Tuberculosis: A Potential Role of Probiotics, and Postbiotics. Front Nutr. 2021;8. doi:10.3389/fnut.2021.626254

3. World Health Organization. WHO global lists of high burden countries for tuberculosis (TB), TB / HIV and TB (MDR / RR-TB). Published online 2021:2021-2025.

4. Enos M, Sitienei J, Ong'ang'o J, et al. Kenya tuberculosis prevalence survey 2016: Challenges and opportunities of ending TB in Kenya. PLoS One. 2018;13(12):1-19. doi:10.1371/journal.pone.0209098

5. Bakhtiar Z, Mirjalili MH. Long-term cell suspension culture of Thymus persicus (Lamiaceae): A novel approach for the production of anti-cancer triterpenic acids. Ind Crops Prod. 2022;181:114818. doi:https://doi.org/10.1016/j.indcrop.2022.114818

6. Gurib-Fakim A. Medicinal plants: Traditions of yesterday and drugs of tomorrow. Mol Aspects Med. 2006;27(1):1-93. doi:https://doi.org/10.1016/j.mam.2005.07.008

7. Kimondo J, Miaron J, Mutai P, Njogu P. Ethnobotanical survey of food and medicinal plants of the Ilkisonko Maasai community in Kenya. J Ethnopharmacol. 2015;175:463-469. doi:10.1016/j.jep.2015.10.013

8. Ruano P, Delgado LL, Picco S, et al. We are IntechOpen , the world ' s leading publisher of Open Access books Built by scientists , for scientists TOP 1 %. Intech. 2016;(tourism):13.

9. Moyo M, Aremu AO. Nutritional, phytochemical and diverse health-promoting qualities of Cleome gynandra. Crit Rev Food Sci Nutr. 2020;0(0):1-18. doi:10.1080/10408398.2020.1867055

10. Wang M, Guan X, Chi Y, Robinson N, Liu JP. Chinese herbal medicine as adjuvant treatment to chemotherapy for multidrug-resistant tuberculosis (MDR-TB): A systematic review of randomised clinical trials. Tuberculosis.

2015;95(4):364-372. doi:https://doi.org/10.1016/j.tube.2015.03.003

11. Orodho JA, Kirimuhuzya C, Otieno JN, Magadula JJ, Okemo P. Local management of tuberculosis by traditional medicine practitioners in Lake Victoria region. Open Complementary Medicine Journal. 2011;3:1-9. doi:10.2174/1876391X01103010001

12. Obakiro SB, Kiprop A, Kowino I, et al. Ethnobotany, ethnopharmacology, and phytochemistry of traditional medicinal plants used in the management of symptoms of tuberculosis in East Africa: A systematic review. Trop Med Health. 2020;48(1):1-21. doi:10.1186/S41182-020-00256-1/FIGURES/5

13. Okello S V, Nyunja RO, Netondo GW, Onyango JC. Ethnobotanical study of medicinal plants used by sabaots of Mt. Elgon Kenya. African Journal of Traditional, Complementary and Alternative Medicines. 2010;7(1):1-10. doi:10.4314/ajtcam.v7i1.57223

14. Kapupara PP, Dholakia SP, Patel VP, Suhagia BN. Journal of Chemical and Pharmaceutical Research preparations. J Chem Pharm Res. 2011;3(4):287-294.

15. Oloyede GK, Ogunlade AO. Phytochemical Screening, Antioxidant, Antimicrobial and Toxicity Activities of Polar and Non-Polar Extracts of Albizia zygia (DC) Stem-Bark. Annual Review & Research in Biology. 2013;3(4):1020-1031.

16. Olukanni OD, Lugard E, Emmanuel E, Olukanni AT, Ayoade F. activities of Albizia zygia (DC) J . F . mebr and the evaluation of its phytochemical constituents. 2020;8(4):317-323.

17. Avoseh ON, Mtunzi FM, Ogunwande IA, Ascrizzi R, Guido F. Albizia lebbeck and Albizia zygia volatile oils exhibit anti-nociceptive and anti-inflammatory properties in pain models. J Ethnopharmacol. 2021;268(July 2020):113676. doi:10.1016/j.jep.2020.113676

18. Abotsi WKM, Lamptey SB, Afrane S, Boakye-Gyasi E, Umoh RU, Woode E. An evaluation of the anti-inflammatory, antipyretic and analgesic effects of hydroethanol leaf extract of albizia zygia in animal models. Pharm Biol. 2017;55(1):338-348. doi:10.1080/13880209.2016.1262434

19. Koagne RR, Annang F, Cautain B, et al. Cytotoxycity and antiplasmodial activity of phenolic derivatives from Albizia zygia (DC.) J.F. Macbr. (Mimosaceae). BMC Complement Med Ther. 2020;20(1):1-8. doi:10.1186/s12906-019-2792-1

20. Fonmboh DJ, Abah ER, Fokunang TE, et al. An Overview of Methods of Extraction, Isolation and Characterization of Natural Medicinal Plant Products in Improved Traditional Medicine Research. Asian Journal of Research in Medical and Pharmaceutical Sciences. 2020;9(August):31-57. doi:10.9734/ajrimps/2020/v9i230152

21. Seidel V. Initial and Bulk Extraction. Natural Products Isolation. Published online 2006:27-46. doi:10.1385/1-59259-955-9:27

22. Mosmann T. Rapid colorimetric assay for cellular growth and survival: application to proliferation and cytotoxicity assays. J Immunol Methods. 1983;65(1-2):55-63.

doi:10.1016/0022-1759(83)90303-4

23. Hendriks BS. Functional pathway pharmacology: Chemical tools, pathway knowledge and mechanistic model-based interpretation of experimental data. Curr Opin Chem Biol. 2010;14(4):489-497. doi:10.1016/J.CBPA.2010.06.167

24. Chaturvedi V, Dwivedi N, Tripathi RP, Sinha S. Evaluation of Mycobacterium smegmatis as a possible surrogate screen for selecting molecules active against multi-drug resistant Mycobacterium tuberculosis. J Gen Appl Microbiol. 2007;53(6):333-337. doi:10.2323/JGAM.53.333

25. Shcherbakov D, Akbergenov R, Matt T, Sander P, Andersson DI, Böttger EC. Directed mutagenesis of mycobacterium smegmatis 16S rRNA to reconstruct the in vivo evolution of aminoglycoside resistance in mycobacterium tuberculosis. Mol Microbiol. 2010;77(4):830-840. doi:10.1111/j.1365-2958.2010.07218.x

26. Webster D, Lee TDG, Moore J, et al. Antimycobacterial screening of traditional medicinal plants using the microplate resazurin assay. Can J Microbiol. 2010;56(6):487-494. doi:10.1139/W10-035

27. Collins L, Franzblau SG. Microplate alamar blue assay versus BACTEC 460 system for high-throughput screening of compounds against Mycobacterium tuberculosis and Mycobacterium avium. Antimicrob Agents Chemother. 1997;41(5):1004-1009.

28. Hsieh MH, Yu CM, Yu VL, Chow JW. Synergy assessed by checkerboard. Diagn Microbiol Infect Dis. 1993;16(4):343-349.

29. Harborne JB. Phytochemical Methods. Published online 1984. doi:10.1007/978-94-009-5570-7

30. Turner DC, Schäfer M, Lancaster S, Janmohamed I, Gachanja A, Creasey J. Sample Collection and Preparation: How Do I Get My Sample Ready for GC-MS Analysis? Gas Chromatography-Mass Spectrometry: How Do I Get the Best Results?. Published online November 28, 2019:1-40. doi:10.1039/9781782629283-00001

31. Gopu C, Chirumamilla P, Daravath SB, Taduri S, Vankudoth S. GC-MS analysis of bioactive compounds in the plant parts of methanolic extracts of Momordica cymbalaria Fenzl. ~ 209 ~ Journal of Medicinal Plants Studies. 2021;9(3):209-218. doi:10.22271/plants.2021.v9.i3c.1289

32. Hevener KE, Zhao W, Ball DM, et al. Validation of Molecular Docking Programs for Virtual Screening against Dihydropteroate Synthase. J Chem Inf Model. 2009;49(2):444. doi:10.1021/CI800293N

33. Prakash P, Vijayasarathi D, Selvam K, Karthi S, Manivasagaperumal R. Pharmacore maping based on docking, ADME/toxicity, virtual screening on 3,5-dimethyl-1,3,4-hexanetriol and dodecanoic acid derivates for anticancer inhibitors. https://doi.org/101080/07391102202001778533. 2020;39(12):4490-4500. doi:10.1080/07391102.2020.1778533

34. Durán-Iturbide NA, Díaz-Eufracio BI, Medina-Franco JL. In Silico ADME/Tox Profiling of Natural Products: A Focus on BIOFACQUIM. ACS Omega. 2020;5(26):16076-

16084. doi:10.1021/ACSOMEGA.0C01581

35. Mishra P, Singh U, Pandey CM, Mishra P, Pandey G. Application of Student's t-test, Analysis of Variance, and Covariance. Ann Card Anaesth. 2019;22(4):407. doi:10.4103/ACA.ACA_94_19

36. Obakiro SB, Kiprop A, K'Owino I, et al. Phytochemical, Cytotoxicity, and Antimycobacterial Activity Evaluation of Extracts and Compounds from the Stem Bark of Albizia coriaria Welw ex. Oliver. Evidence-based Complementary and Alternative Medicine. 2022;2022. doi:10.1155/2022/7148511

37. Mmushi TJ, Masoko P, Mdee LK, Mokgotho MP, Mampuru LJ, Howard RL. Antimycobacterial evaluation of fifteen medicinal plants in South Africa. African Journal of Traditional, Complementary and Alternative Medicines. 2010;7(1):34-39. doi:10.4314/ajtcam.v7i1.57230

38. Indrayanto G, Putra GS, Suhud F. Validation of in-vitro bioassay methods: Application in herbal drug research. Profiles Drug Subst Excip Relat Methodol. 2021;46:273-307. doi:10.1016/BS.PODRM.2020.07.005

39. Olajuyigbe OO, Afolayan AJ. Synergistic Interactions of Methanolic Extract of Acacia mearnsii De Wild. with Antibiotics against Bacteria of Clinical Relevance. Int J Mol Sci. 2012;13(7):8915. doi:10.3390/IJMS13078915

40. Ndjakou Lenta B, Vonthron-Sénécheau C, Fongang Soh R, et al. In vitro antiprotozoal activities and cytotoxicity of some selected Cameroonian medicinal plants. J Ethnopharmacol. 2007;111(1):8-12. doi:10.1016/J.JEP.2006.10.036

41. Appiah-Opong R, Asante IK, Safo DO, et al. Cytotoxic effects of Albizia zygia (DC) J. F. Macbr, a Ghanaian medicinal plant, against human T-lymphoblast-like leukemia, prostate and breast cancer cell lines. Int J Pharm Pharm Sci. 2016;8(5):392-396. Accessed July 25, 2024. https://pure.ug.edu.gh/en/publications/cytotoxic-effects-of-albizia-zygia-dc-j-f-macbr-a-ghanaian-medici-2

42. Abuzeid N, Kalsum S, Larsson M, et al. Antimycobacterial activity of selected medicinal plants traditionally used in Sudan to treat infectious diseases. J Ethnopharmacol. 2014;157:134-139. doi:10.1016/j.jep.2014.09.020

43. Obakiro SB, Kiprop A, Kowino I, et al. phytochemistry of traditional medicinal plants used in the management of symptoms of tuberculosis in East Africa : a systematic review. 2020;1:1-21.

44. Eldeen IMS, Van Staden J. Antimycobacterial activity of some trees used in South African traditional medicine. South African Journal of Botany. 2007;73(2):248-251. doi:10.1016/J.SAJB.2006.09.004

45. Tafesse G, Mekonnen Y, Makonnen E, Majinda RRT, Bojase-Moleta G, Yeboah SO. Antibacterial activity of crude extracts and pure compounds isolated from Vernonia galamensis leaves. Afr J Pharm Pharmacol. 2018;12(11):136-141. doi:10.5897/AJPP2018.4888

46. Kigondu EM, Njoroge M, Singh K, Njuguna N, Warner DF, Chibale K. Synthesis and synergistic antimycobacterial screening of chlorpromazine and its metabolites. Medchemcomm. 2014;5(4):502-506. doi:10.1039/C3MD00387F

47. Reddy VM, Einck L, Andries K, Nacy CA. In Vitro Interactions between New Antitubercular Drug Candidates SQ109 and TMC207. Antimicrob Agents Chemother. 2010;54(7):2840-2846. doi:10.1128/AAC.01601-09

48. Mar Htay T, Kyi Sann K, Haini H. Comparative Study on Phytochemical Screening and Antioxidant Activity of Aqueous Extract from Various Parts of Bauhinia purpurea. Bioactivities. 2023;2023(1). doi:10.47352/bioactivities.2963-654X.183i

49. Rahgozar N, Khaniki GB, Sardari S. Evaluation of antimycobacterial and synergistic activity of plants selected based on cheminformatic parameters. Iran Biomed J. 2018;22(6):401-407. doi:10.29252/.22.6.401

50. Obonga WO, Uzor PF, Ekwealor EO, Nwabuko SC. Comparative phytochemical, antioxidant and antimicrobial properties of Ficus capensis, Aristolochia ringens, Albizia zygia and Lannea welwitschii. Dhaka University Journal of Pharmaceutical Sciences. 2017;16(2):147-157. doi:10.3329/dujps.v16i2.35249

51. Chen Z, Liu Q, Zhao Z, et al. Effect of hydroxyl on antioxidant properties of 2,3-dihydro-3,5-dihydroxy-6-methyl-4 H-pyran-4-one to scavenge free radicals. RSC Adv. 2021;11(55):34456-34461. doi:10.1039/D1RA06317K

52. Zhao F, Wang P, Lucardi RD, Su Z, Li S. Natural sources and bioactivities of 2,4-di-tert-butylphenol and its analogs. Toxins (Basel). 2020;12(1):1-26. doi:10.3390/toxins12010035

53. Abdassalam AFSH, Deniz NG, Sayil C, et al. A novel series of (E)-S and (E)-N,S-polyhalonitrobutadiene analogues: design and evaluation of antibacterial and antifungicidial activity. Journal of Chemical Sciences 2021 133:4. 2021;133(4):1-10. doi:10.1007/S12039-021-01986-3

54. Barbuceanu SF, Almajan GL, Saramet I, Draghici C, Tarcomnicu AI, Bancescu G. Synthesis, characterization and evaluation of antibacterial activity of some thiazolo[3,2-b][1,2,4]triazole incorporating diphenylsulfone moieties. Eur J Med Chem. 2009;44(11):4752-4757. doi:10.1016/J.EJMECH.2009.06.021

55. Narender P, Srinivas U, Ravinder M, et al. Synthesis of multisubstituted quinolines from Baylis-Hillman adducts obtained from substituted 2-chloronicotinaldehydes and their antimicrobial activity. Bioorg Med Chem. 2006;14(13):4600-4609. doi:10.1016/j.bmc.2006.02.020

56. Upadhayaya RS, Vandavasi JK, Vasireddy NR, Sharma V, Dixit SS, Chattopadhyaya J. Design, synthesis, biological evaluation and molecular modelling studies of novel quinoline derivatives against Mycobacterium tuberculosis. Bioorg Med Chem. 2009;17(7):2830-2841. doi:10.1016/J.BMC.2009.02.026

57. Jyoti MA, Nam KW, Jang WS, et al. Antimycobacterial activity of methanolic plant extract of Artemisia capillaris containing ursolic acid and hydroquinone against Mycobacterium tuberculosis. Journal of Infection and Chemotherapy. 2016;22(4):200-208. doi:10.1016/J.JIAC.2015.11.014

58. Huang S, Chen X, Yan R, Huang M, Chen D. Isolation, Identification and Antibacterial Mechanism of the Main Antibacterial Component from Pickled and Dried Mustard (Brassica juncea Coss. var. foliosa Bailey). Molecules. 2022;27(8). doi:10.3390/molecules27082418

59. Olivia NU, Goodness UC, Obinna OM. Phytochemical profiling and GC-MS analysis of aqueous methanol fraction of Hibiscus asper leaves. Future Journal of Pharmaceutical Sciences 2021 7:1. 2021;7(1):1-5. doi:10.1186/S43094-021-00208-4

60. Venugopala KN, Chandrashekharappa S, Deb PK, et al. Anti-tubercular activity and molecular docking studies of indolizine derivatives targeting mycobacterial InhA enzyme. J Enzyme Inhib Med Chem. 2021;36(1):1472. doi:10.1080/14756366.2021.1919889

61. Tanina A, Wohlkönig A, Soror SH, et al. A comprehensive analysis of the protein-ligand interactions in crystal structures of Mycobacterium tuberculosis EthR. Biochim Biophys Acta Proteins Proteom. 2019;1867(3):248-258. doi:10.1016/J.BBAPAP.2018.12.003

62. Engohang-Ndong J, Baillat D, Aumercier M, et al. EthR, a repressor of the TetR/CamR family implicated in ethionamide resistance in mycobacteria, octamerizes cooperatively on its operator. Mol Microbiol. 2004;51(1):175-188. doi:10.1046/J.1365-2958.2003.03809.X

63. Mugumbate G, Mendes V, Blaszczyk M, et al. Target identification of Mycobacterium tuberculosis phenotypic hits using a concerted chemogenomic, biophysical, and structural approach. Front Pharmacol. 2017;8(SEP). doi:10.3389/fphar.2017.00681

64. Durán-Iturbide NA, Díaz-Eufracio BI, Medina-Franco JL. In Silico ADME/Tox Profiling of Natural Products: A Focus on BIOFACQUIM. ACS Omega. 2020;5(26):16076-16084. doi:10.1021/ACSOMEGA.0C01581/SUPPL_FILE/AO0C01581_SI_001.PDF

65. Elmeliegy M, Vourvahis M, Guo C, Wang DD. Effect of P-glycoprotein (P-gp) Inducers on Exposure of P-gp Substrates: Review of Clinical Drug-Drug Interaction Studies. Clin Pharmacokinet. 2020;59(6):699-714. doi:10.1007/S40262-020-00867-1

66. Krüger A, Maltarollo VG, Wrenger C, et al. ADME Profiling in Drug Discovery and a New Path Paved on Silica. Drug Discovery and Development - New Advances. Published online May 2, 2019. doi:10.5772/INTECHOPEN.86174

67. Waring RH. Cytochrome P450: genotype to phenotype. Xenobiotica. 2020;50(1):9-18. doi:10.1080/00498254.2019.1648911

Peer Reviewed